



Sterically Hindered 2-(2'-Hydroxyphenyl)benzoxazole (HBO) Emitters: Synthesis, Spectroscopic Studies, and Theoretical Calculations

Timothée Stoerkler, Thibault Pariat, Adèle Laurent, Denis Jacquemin, Gilles Ulrich, Julien Massue

► To cite this version:

Timothée Stoerkler, Thibault Pariat, Adèle Laurent, Denis Jacquemin, Gilles Ulrich, et al.. Sterically Hindered 2-(2'-Hydroxyphenyl)benzoxazole (HBO) Emitters: Synthesis, Spectroscopic Studies, and Theoretical Calculations. *European Journal of Organic Chemistry*, 2022, 2022 (30), pp.e202200661. 10.1002/ejoc.202200661 . hal-03853150v2

HAL Id: hal-03853150

<https://cnrs.hal.science/hal-03853150v2>

Submitted on 8 Mar 2023

HAL is a multi-disciplinary open access archive for the deposit and dissemination of scientific research documents, whether they are published or not. The documents may come from teaching and research institutions in France or abroad, or from public or private research centers.

L'archive ouverte pluridisciplinaire **HAL**, est destinée au dépôt et à la diffusion de documents scientifiques de niveau recherche, publiés ou non, émanant des établissements d'enseignement et de recherche français ou étrangers, des laboratoires publics ou privés.

Excellence in Chemistry Research

Announcing our new flagship journal

- Gold Open Access
- Publishing charges waived
- Preprints welcome
- Edited by active scientists



Meet the Editors of *ChemistryEurope*



Luisa De Cola
Università degli Studi
di Milano Statale, Italy



Ive Hermans
University of
Wisconsin-Madison, USA



Ken Tanaka
Tokyo Institute of
Technology, Japan

Sterically Hindered 2-(2'-Hydroxyphenyl)benzoxazole (HBO) Emitters: Synthesis, Spectroscopic Studies, and Theoretical Calculations

Timothée Stoerkler,^[a] Thibault Pariat,^[a] Adèle D. Laurent,^[b] Denis Jacquemin,^{*,[b]} Gilles Ulrich,^[a] and Julien Massue^{*,[a]}

We describe various synthetic pathways to introduce sterically hindered substituents (mesityl, 2,4,6-triisopropylphenyl, anthracene) to the proton donor side of excited-state intramolecular proton transfer (ESIPT)-capable 2-(2'-hydroxyphenyl)benzoxazole (HBO) fluorophores. Two original synthetic approaches were investigated in order to synthesize seven HBO derivatives. Optimization studies concluded that electron rich and bulky phosphine ligands are required to ensure completion

of the Suzuki-Miyaura cross-coupling reaction involving a bulky aromatic boronic acid. The photophysical properties of all dyes revealed a strong influence of the nature of the solvent on the optical properties, as protic solvents tend to stabilize enol tautomers and induce dual emission. Our studies confirmed that, unlike the majority of organic dyes, ESIPT fluorophores do not undergo π -stacking in the solid-state. The nature of the excited-states was explored by *ab initio* calculations.

Introduction

2-(2'-Hydroxyphenyl)benzoxazole (HBO) derivatives are well-known versatile organic fluorophores whose facile synthesis enables the investigation of the impact of incremental structural inputs on their photophysical properties. They are notably famous for displaying excited-state intramolecular proton transfer (ESIPT) process, owing to the presence of a strong six-membered intramolecular hydrogen bond in their structure.^[1–4] ESIPT is a phototautomerization reaction which turns, in most cases, an excited enol (E^*) derivative into the corresponding keto (K^*) upon proton migration and structural reorganization. The radiative relaxation of this excited keto species to the ground-state leads to a strongly red-shifted fluorescence emission (Figure 1).^[5] The understanding and modulation of ESIPT photophysics was deeply investigated since ESIPT-capable dyes like HBO derivatives typically show enhanced photo-

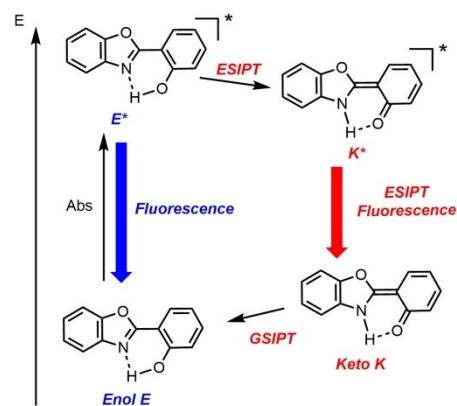


Figure 1. Representation of the ESIPT process in 2-(2'-Hydroxyphenyl)benzoxazole (HBO) derivatives. GS IPT = ground-state intramolecular proton transfer.

stability, strong solid-state emission, as well as environment-sensitive optical properties.^[6–9] As a result, a rich database of optimized ESIPT dyes has been engineered and applied to numerous applications, including optoelectronic devices,^[10–11] bio-sensing or -imaging,^[12–13] security inks,^[14] white luminescence^[15–17] along with various luminescent displays.^[18] These attractive derivatives are mostly reported as solid-state emitters since, unlike the majority of organic compounds, ESIPT greatly limits aggregation-caused quenching (ACQ) phenomenon in solid. In solution, proton transfer processes such as ESIPT might trigger a large panel of excited-state dynamics, including deactivation through accessible conical intersection (CI) and hence strong fluorescence quenching. Several studies have consequently reported synthetic strategies to increase solution-state fluorescence and engineer dual-state emission ESIPT fluorophores displaying intense emission in both solution and solid.^[19] For example, enhancing molecular rigidity in derivatives

[a] T. Stoerkler, Dr. T. Pariat, Dr. G. Ulrich, Dr. J. Massue
Institut de Chimie et Procédés pour l'Energie,
l'Environnement et la Santé (ICPEES),
Equipe Chimie Organique pour la Biologie, les Matériaux et l'Optique
(COMBO), UMR CNRS 7515, Ecole Européenne de Chimie, Polymères et
Matériaux (ECPM),
25 Rue Becquerel, 67087 Strasbourg Cedex 02, France
E-mail: massue@unistra.fr

[b] Dr. A. D. Laurent, Prof. Dr. D. Jacquemin
CEISAM, UMR CNRS 6230,
Nantes University,
Nantes 44322, France
E-mail: Denis.Jacquemin@univ-nantes.fr

Supporting information for this article is available on the WWW under
<https://doi.org/10.1002/ejoc.202200661>

© 2022 The Authors. European Journal of Organic Chemistry published by
Wiley-VCH GmbH. This is an open access article under the terms of the
Creative Commons Attribution Non-Commercial NoDerivs License, which
permits use and distribution in any medium, provided the original work is
properly cited, the use is non-commercial and no modifications or adap-
tations are made.

like imidazo[1,2-*f*]phenanthridine^[20] or 3,5-ethynyl-hydroxy-phenyl-benzazole^[21–23] has appeared as a straightforward synthetic trick to reduce non-radiative deactivations through the well-known “twisting CI”. A recent alternative includes the incorporation of pyridinium units onto the HBO scaffold to stabilize the K* species by resonance effects, leading to drastic enhancement of fluorescence intensity in solution.^[24]

In the past years, we have been actively developing synthetic possibilities to modulate the strength of the ESIPT process, correlated to the relative excited-state energies of the tautomers in order to shed additional light onto the photo-physics of ESIPT dyes and obtain original optical profiles. Molecular engineering studies around the HBO core notably led the observation of dual E*/K* emission,^[25] the full frustration of the proton transfer upon extension of π -conjugation^[26] or the stabilization of fluorescent anionic species originating from deprotonation in lieu of ESIPT.^[27] In this context, we wish to report herein on our synthetic efforts to introduce sterically hindered arenes, functionalized by bulky substituents (mesityl (Mes), 2,4,6-triisopropylphenyl (Tip), anthracene (Ant)) on the phenolic side of HBO dyes, in order to assess their influence on the photophysical properties. It is of fundamental interest to study the influence of increasing bulkiness on HBO dyes, since fluorescence intensity amplification upon introduction of voluminous groups for various dyes can be found in the literature.^[28,29] The synthetic targets described herein are displayed on Figure 2 and required the introduction at the 3, 5 or 3,5 positions of the phenol ring of the aforementioned bulky

arenes but also aliphatic groups such as tertio-butyl or tolyl, for references and comparison purposes.

Results and Discussion

Different synthetic routes were investigated in order to provide the various dyes presented on Figure 2.

The synthesis of **HBO-5-Mes** and **HBO-5-Ant** is presented on Scheme 1. Inspired by a recent publication describing the Pd-catalyzed formation of C–C bonds on bulky aromatic moieties,^[30] HBO dyes **HBO-5-Mes** and **HBO-5-Ant** were obtained in four steps. 5-BrHBO **1** is straightforwardly synthesized by condensation in ethanol between 2-aminophenol and 5-Bromo-salicylaldehyde, followed by oxidation in CH₂Cl₂ with a slight excess of DDQ. The phenol group in HBO **1** is then protected with methoxy, followed by cuprate formation and subsequent Pd-catalyzed cross-coupling at 0 °C. A final deprotection step with boron tribromide in dichloromethane affords the desired compounds in an overall 24 and 20% yield respectively, as white powders.

This fastidious protocol, along with the moderate global yields of the desired dyes prompted us to find synthetic alternatives to access the targets. We decided to focus our optimization studies in the Suzuki-Miyaura cross-coupling reaction between the commercially available coupling partners 3,5-dihalogenosalicylaldehyde and 2,4,6-trimethylboronic acid to yield 3,5-dimesitylsalicylaldehyde **2** (Table 1).

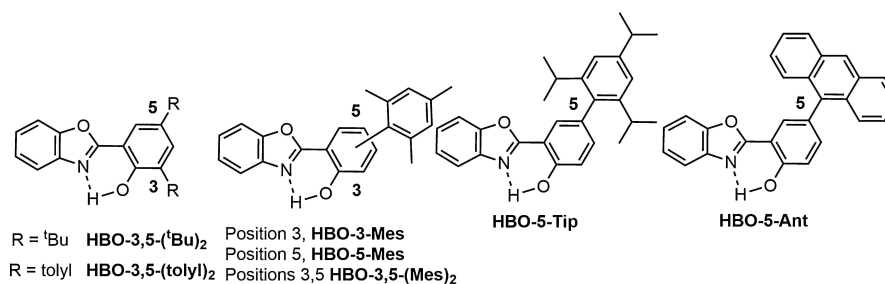
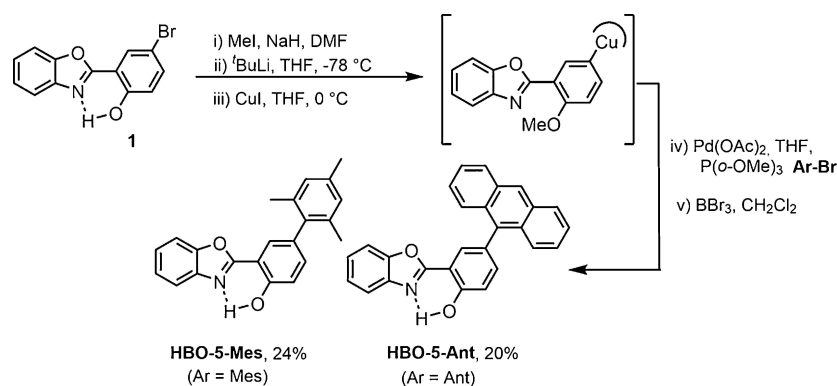
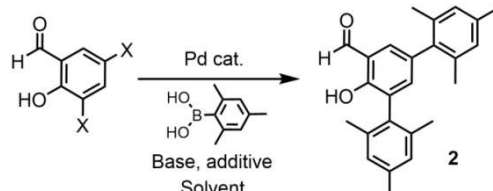


Figure 2. Sterically hindered HBO dyes studied in this article.

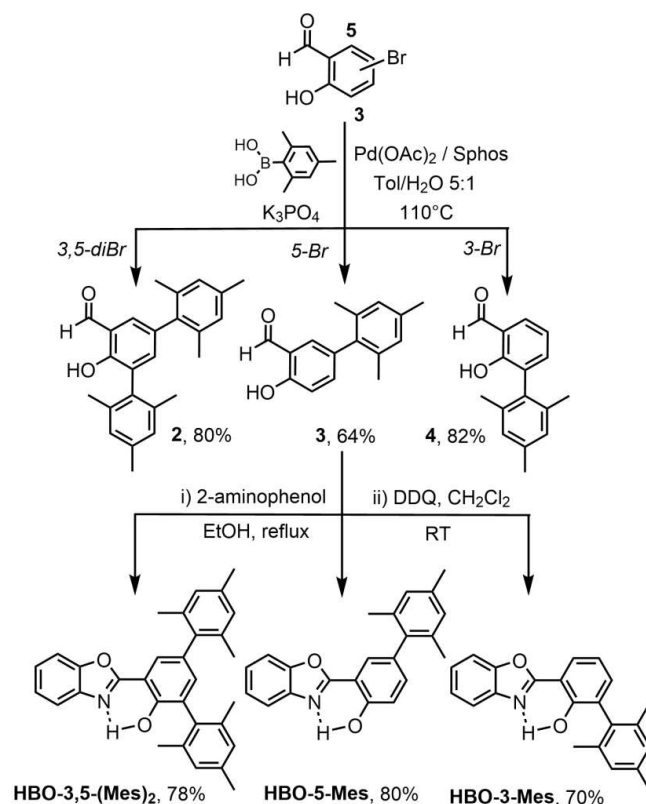


Scheme 1. Synthesis of HBO-5-Mes and HBO-5-Ant.

Table 1. Optimization conditions for the Suzuki-Miyaura cross-coupling for the synthesis of salicylaldehyde **2**.

							
Entry	X	Pd Cat.	Base	Additive	T [°C]	Solvent	Yield
1	I	Pd(PPh ₃) ₂ Cl ₂	K ₂ CO ₃	–	95 °C	Dioxane/H ₂ O 3:1	no reaction
2	Br	Pd(PPh ₃) ₂ Cl ₂	K ₂ CO ₃	–	95 °C	Dioxane/H ₂ O 3:1	no reaction
3	Br	Pd(PPh ₃) ₂ Cl ₂	K ₂ CO ₃	–	95 °C	Dioxane/H ₂ O 4:1	no reaction
4	Br	Pd(PPh ₃) ₂ Cl ₂	K ₂ CO ₃	–	95 °C	Tol/EtOH 2:1	no reaction
5	Br	Pd(PPh ₃) ₂ Cl ₂	K ₂ CO ₃	–	95 °C	Tol/EtOH/H ₂ O 9:4:1	no reaction
6	Br	Pd(PPh ₃) ₂ Cl ₂	K ₂ CO ₃	–	95 °C	DME/H ₂ O 4:1	no reaction
7	Br	Pd(PPh ₃) ₂ Cl ₂	K ₂ CO ₃	–	95 °C	DMF/H ₂ O 4:1	no reaction
8	Br	Pd(PPh ₃) ₂ Cl ₂	K ₂ CO ₃	CuI	95 °C	Dioxane /H ₂ O 2:1	no reaction
9	Br	Pd(OAc) ₂ /Xphos	K ₂ CO ₃	–	95 °C	Dioxane /H ₂ O 2:1	no reaction
10	Br	Pd(OAc) ₂ /Sphos	K ₃ PO ₄	–	110 °C	Tol/H ₂ O 5:1	80%
11	Br	Pd(OAc) ₂ /Xphos	K ₃ PO ₄	–	110 °C	Tol/H ₂ O 5:1	50%
12	Br	Pd(PPh ₃) ₂ Cl ₂	K ₃ PO ₄	–	110 °C	Tol/H ₂ O 5:1	no reaction

In all examples described in Table 1, three equivalents of 2,4,6-trimethylboronic acid, four equivalents of base, and 5 mol. % of catalyst were systematically used. The first reaction conditions modification involve the nature of the halogen atoms on the salicylaldehyde derivative which is an important parameter for the oxidative addition step (entries 1 and 2). Neither iodine nor bromine functionalized derivatives provided any traces of the desired salicylaldehyde **2**, using standard Suzuki-Miyaura cross-coupling conditions, that are, Pd(PPh₃)₂Cl₂, K₂CO₃ in a 3:1 mixture of dioxane/H₂O. The nature of the solvent was then modified in order to prevent solubility issues of the starting reactants or intermediate species. Increase of the ratio of dioxane/H₂O mixture (entry 3) or use of toluene (entries 4 and 5), DME (entry 6) or DMF (entry 7) did not provide observation of salicylaldehyde **2** in crude ¹H NMR spectra. Addition of copper (I) iodide as additive in the reaction medium was no more fruitful in obtaining of **2** (entry 8). Then, we decided to change the nature of the catalytic system by using Pd(II) acetate and an electron-rich phosphine ligand. Even though the use of 2-dicyclohexylphosphino-2,4,6-triisopropylbiphenyl (Xphos) ligand in dioxane/H₂O mixture did not provide the expected compound **2**, electron-rich 2-dicyclohexylphosphino-2,6-dimethoxybiphenyl (Sphos) ligand combined with potassium phosphate as a base at 110 °C in toluene/H₂O mixture appeared to be much more efficient. These Suzuki-Miyaura reaction conditions, inspired by a reported procedure,^[31] allowed the preparation of salicylaldehyde **2** in 80% yield after purification on silica gel column chromatography. Replacement of Sphos by Xphos, under the same other coupling conditions only yielded 50% of **2** (entry 11). The same reaction conditions, as in entry 10 were then applied to mono-substituted bromo salicylaldehydes, at the 3- and the 5-position to yield derivatives **3** and **4** in good to excellent yields (64–82%), highlighting the broad applicability of these reaction conditions to introduce bulky substituents on arene cores (Scheme 2).



Scheme 2. Synthesis of HBO-3,5-(Mes)₂, HBO-5-Mes and HBO-3-Mes.

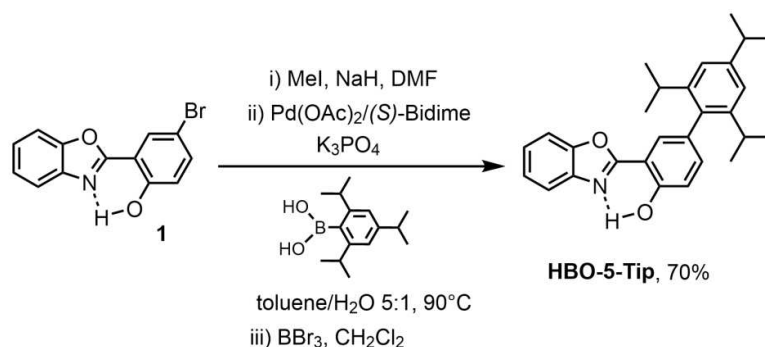
The corresponding HBO derivatives were synthesized from salicylaldehydes **2–4**, using standard protocols, *i.e.*, condensation with 2-aminophenol in refluxing ethanol followed by an oxidation step using 2,3-dichloro-5,6-dicyano-1,4-benzoquinone (DDQ) in dichloromethane.^[21] HBO-3,5-(Mes)₂, HBO-5-Mes and HBO-3-Mes were obtained as white powders in 70–80% yield,

which overall represents a significant improvement as compared to the synthetic protocol described in Scheme 1.

To expand the number of examples in this family of dyes, we also tried to introduce 2,4,6-triisopropylphenyl (Tip) group at the 3- and 5-position of the salicylaldehyde core using the coupling conditions optimized in Table 1, but with no success (Table S1). Inspired by a publication describing catalytic couplings of sterically demanding arenes,^[32] we decided to change the phosphine ligand and use oxazole-based (*S*)-bidime in the catalytic system. Although it appeared unsuccessful on 3,5-dibromo salicylaldehyde, we tried it on the methoxy protected version of HBO 1, where it successfully led to the

completion of the reaction and afforded HBO-5-Tip in an overall 70 % yield after methoxy deprotection (Scheme 3).

The photophysical properties in solution (toluene, ethanol) and in the solid-state (KBr pellet), of all synthesized dyes, along with the data for the unsubstituted HBO used as benchmark are listed in Table S2. The absorption and emission spectra in solution for HBO, HBO-3,5-(*t*Bu)₂, HBO-3,5-(tolyl)₂, HBO-5-Mes, HBO-3-Mes, HBO-3,5-(Mes)₂ and HBO-5-Tip are presented in Figure 3, while those of HBO-5-Ant can be found on Figure 4. Emission spectra of all dyes in the solid-state are displayed on Figure 5.



Scheme 3. Synthesis of HBO-5-Tip.

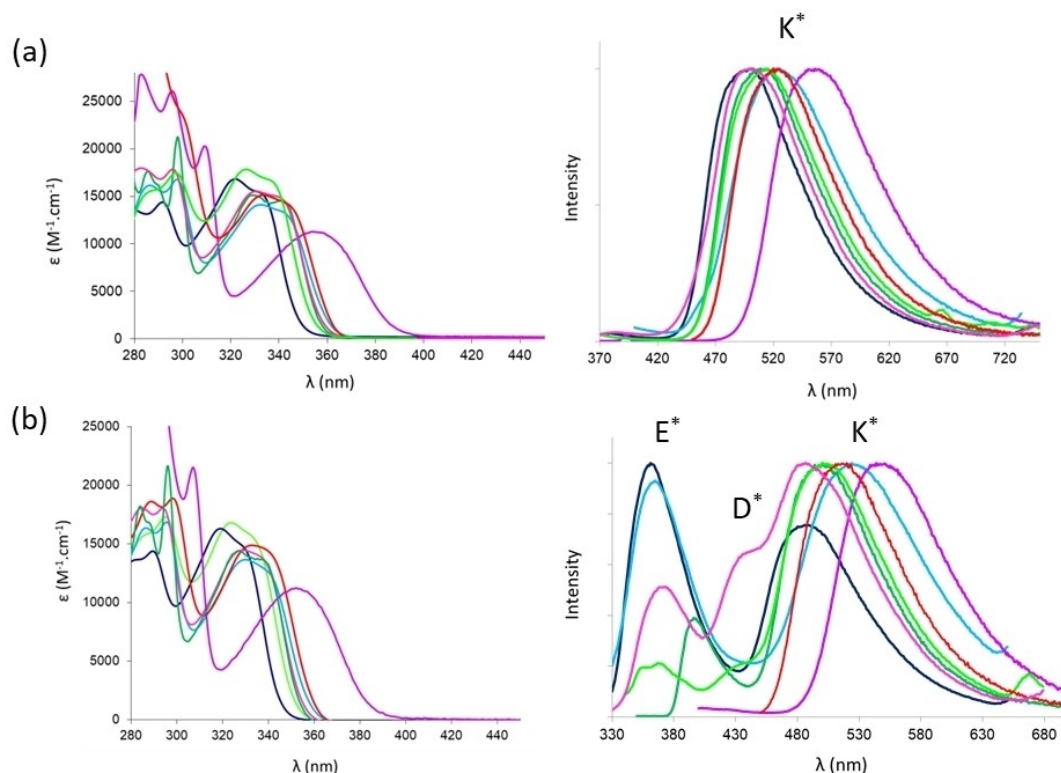


Figure 3. Absorption (left) and emission (right) spectra of HBO (navy blue), HBO-3,5-(*t*Bu)₂ (blue), HBO-3,5-(tolyl)₂ (purple), HBO-5-Mes (green), HBO-3-Mes (light green), HBO-3,5-(Mes)₂ (red) and HBO-5-Tip (pink) in (a) toluene and (b) ethanol.

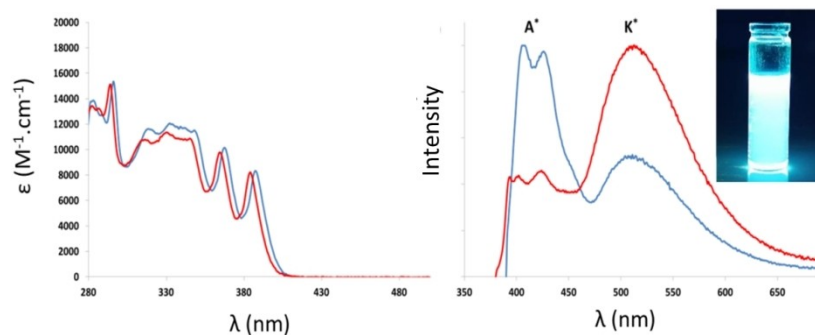


Figure 4. Absorption (left) and Emission (right) spectra of **HBO-5-Ant** in toluene (blue) and ethanol (red), at 25 °C. Insert: Photograph of a solution of **HBO-5-Ant** in toluene under irradiation from a bench UV-lamp ($\lambda_{\text{exc}} = 365$ nm).

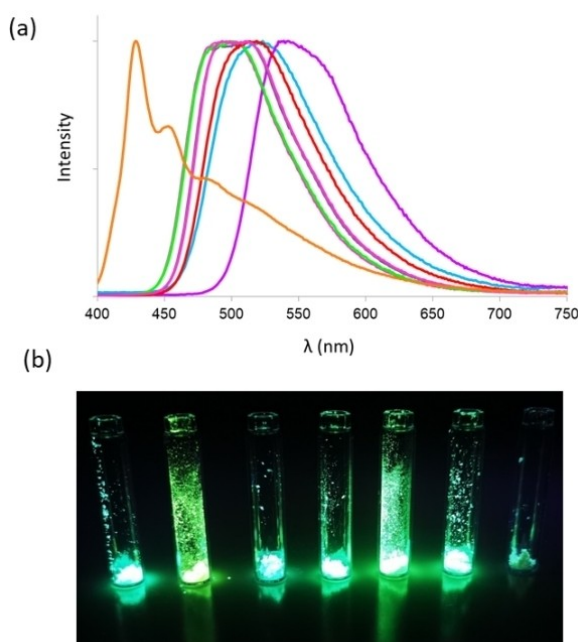


Figure 5. (a) Emission spectra of **HBO** (navy blue), **HBO-3,5-(tBu)₂** (blue), **HBO-3,5-(tolyl)₂** (purple), **HBO-5-Mes** (green), **HBO-3-Mes** (light green), **HBO-3,5-(Mes)₂** (red), **HBO-5-Tip** (pink) and **HBO-5-Ant** (orange) in the solid-state as embedded in KBr pellets (1 % wt) (concentration around 10^{-5} M), and (b) Photographs of **HBO**, **HBO-3,5-(tBu)₂**, **HBO-5-Mes**, **HBO-3-Mes**, **HBO-3,5-(Mes)₂**, **HBO-5-Tip** and **HBO-5-Ant** as powders under irradiation from a bench UV-lamp ($\lambda_{\text{exc}} = 365$ nm).

All dyes, except **HBO-3,5-(tolyl)₂** show highly similar absorption spectra, consisting of two absorption bands (Figure 3a and (Figure 3b). The first band, intense and structured is found below 320 nm and can be ascribed to the $\pi \rightarrow \pi^*$ transitions of the benzoxazole units (Table S2). The second band, rather broad and unstructured, located between 326 and 332 nm in toluene and 319 and 333 nm in ethanol can be attributed to the $S_0 \rightarrow S_1$ transition characteristic of the HBO dye. Molar absorption coefficients are in the $11,400\text{--}17,800\text{ M}^{-1}\text{cm}^{-1}$ range, consistent with data reported for similar compounds.^[21–24] **HBO-3,5-(tolyl)₂** dye stands out in the series with a recorded bathochromic shift of the maximum absorption

wavelength ($\lambda_{\text{abs}} = 352\text{--}354$ nm), highlighting a stronger electronic connection between the tolyl unit and the HBO core, which is also found in the simulations (*vide infra*). **HBO-5-Ant** presents absorption profiles in toluene and ethanol typically observed for polyaromatic-containing fluorophores, *i.e.* intense vibronic bands ($\lambda_{\text{abs}} = 332, 367$ and 387 nm in toluene) located in the UV region (Figure 4), indicating that the anthracene moiety is significantly involved in the lowest excited state(s).

After photoexcitation in the lower energy band ($\lambda_{\text{exc}} = 310\text{--}350$ nm), an intense emission is observed, consisting of one or two emission bands, corresponding to the single decay of K^* or dual E^*/K^* species (Figure 3a and Figure 3b). The dual emission profile is only observed in ethanol, as it is well-known that protic solvents are able to stabilize excited enol tautomers through intermolecular H-bonding interactions in ESIPT structures.^[33]

In toluene, all dyes display a single K^* band whose maximum emission wavelength spans from 499 to 524 nm, depending on substitution, with the exception of **HBO-3,5-(tolyl)₂** ($\lambda_{\text{em}} = 550$ nm) (Table S2). These data are in alignment with the emission of unsubstituted **HBO** ($\lambda_{\text{em}} = 499$ nm), consistent with the absence of rotation owing to the presence of mesityl or tip substitution at the 3, 5 or 3,5 position of the phenol. These data are also consistent with theoretical simulations (*vide infra*). In ethanol, a dual E^*/K^* profile is observed in all cases with the notable exception of **HBO-3,5-(Mes)₂**. Moreover, for **HBO-3-Mes** and **HBO-3,5-Tip**, an additional third band is observed, located between E^* and K^* leading to a triple emission (Figure 3b). Based on previous reported studies on the photophysics of related HBO derivatives, this band can be unambiguously ascribed to the deprotonated species D^* , originating from a competitive deprotonation process in the excited state.^[22,27,33]

All calculated photoluminescent calculated quantum yields (PLQY) lie within the same range as the HBO reference, *i.e.* 1–6% in toluene and 1–3% in ethanol, highlighting the absence of interaction between the HBO core and the hindered phenolic substitution. It is worth noting that **HBO-3,5-(tolyl)₂** appears to be the brightest in the series (QY = 11% in toluene). Fluorescent lifetimes are all in the nanosecond range, consistent with the extremely fast organic fluorescence. These low quantum yields

are a common feature among ESIPT dyes, as proton transfer triggers strong vibrational relaxations, at the origin of enhanced non-radiative deactivations.

After photoexcitation at 350 nm, **HBO-5-Ant** displays two distinct broad and structured emission bands, both in toluene and ethanol with maxima ranging from 390 to 425 nm for the first band and at 510 nm for the second one. The first band is assigned to the anthracene antenna (A^*) while the second one is characteristic of the K^* emission, as a result of ESIPT. A notable difference between the optical properties observed in toluene and those recorded in ethanol is the A^*/K^* intensity ratio; the K^* and A^* being the most intense bands in toluene and ethanol, respectively. A tentative explanation resides in the difference of viscosity between the two solvents (0.53 and 0.97 mPa·s for toluene and ethanol, respectively).^[34] The enhanced viscosity of ethanol leads to a stabilization of the A^* species. The photophysical data determined for **HBO-5-Ant** are in line with a reported benzimidazole analogue, where the authors evidence a rotation in the excited state of the anthracene sub-unit to yield a quasi-planar conformation.^[35]

All dyes described herein display intense emission as amorphous powders under irradiation with a UV-lamp ($\lambda_{\text{exc}} = 365$ nm) (Figure 5b). The photophysical properties in the solid-state were recorded as embedded in potassium bromide (KBr) pellets. As expected for sterically-encumbered derivatives, the maximum emission wavelengths are rather similar to those observed in solution in toluene, with maxima ranging from 501 to 527 nm. Notably, all dyes display a single strongly red-shifted (K^*) band, evidencing a quantitative ESIPT process in the solid-state. **HBO-3,5-tolyl** stands out in the series with a bathochromically shifted emission band ($\lambda_{\text{em}} = 539$ nm), consistent with its absorption. **HBO-5-Ant** is the only dye to display a dual A^*/K^* , although the K^* band seems to only appear as a shoulder ($\lambda_{\text{em}} = 429/520$ nm) (Figure 5a).

The PLQY, recorded as absolute, with an integration sphere fitted to a spectrophotometer, are recorded as much higher as those recorded in solution, regardless of the solvent ($QY = 45\text{--}68\%$). This feature, well-known for ESIPT dyes, is attributed to a restriction of molecular motions in the excited-state, and in particular the rotation around the central double bond of the K^* form.^[7] However, no significant increase of the PLQY value is observed for the sterically hindered HBO series, as compared to the unsubstituted HBO reference, which is a clear indication of the complete lack of π -stacking in ESIPT-capable fluorophores.

We have performed theoretical calculations to probe the nature of the electronic excited states (see the SI for details). Given that we rely on a continuum model for treating the environment, only toluene was considered. Key results are displayed in Table 2. We will discuss the trickier case of **HBO-5-Ant** separately (*vide infra*). For all the other dyes, the lowest excited-state present the usual topology of ESIPT dyes derived from HBOs (see density difference plots in Figure S5.1). The computed vertical transition wavelengths are similar for all compounds (in the 310–318 nm range), but for **HBO-3,5-(tolyl)**₂ whose absorption is red-shifted ($\lambda_{\text{abs}} = 334$ nm) consistently with the experimental trends. This can be straightforwardly explained by the density difference plots of Figure S5.1, i.e. the

Table 2. Main computed data (in toluene) for all compounds: vertical absorption and emission wavelengths (nm) and difference of free energies between the enol and keto tautomers in the excited state (eV). All values are CC2-corrected TD-DFT data (see the Supporting Information).

Dye	$\lambda_{\text{vert-abs}}$ [nm]	$\lambda_{\text{vert-em}} (E^*)$ [nm]	$\lambda_{\text{vert-em}} (K^*)$ [nm]	$\Delta E (K^*-E^*)$ [eV]
HBO-3,5-(tBu) ₂	318	371	500	−0.261
HBO-3,5-(tolyl) ₂	334	396	529	−0.203
HBO-5-Mes	313	366	482	−0.223
HBO-3-Mes	310	360	489	−0.262
HBO-3,5-(Mes) ₂	318	375	501	−0.227
HBO-5-Tip	314	365	481	−0.219
HBO-5-Ant	354 and 322	424 ^[a]	484 ^[b]	

[a] Anthracene-based emission (A^*); [b] No clear E^* state could be localized.

tolyl group is involved in the excited state of **HBO-3,5-(tolyl)**₂, providing an improved delocalization, contrary to all other compounds, in which there is a larger dihedral angle between the HBO core and the side groups. For the fluorescence, we could locate true minima for both the E^* and K^* tautomers, yet the latter are systematically more stable by more than 0.2 eV, indicating a very strong driving force for proton transfer, and hence quantitative ESIPT.^[38] This conclusion is also supported by the computed emission wavelengths, which are in the 365–396 nm range for E^* and 481–529 nm range for K^* , the latter obviously better fitting experimental observations. Similar to what was observed for absorption, **HBO-3,5-(tolyl)**₂ shows the most red-shifted emission of the series; a feature consistent with the experimental observations.

For **HBO-5-Ant**, the spectral features are more complex, as the absorption of the anthracene and the HBO core are relatively close in energy. The lowest excited state is clearly localized on the anthracene moiety according to the calculation (Figure S5.2). Theory finds a rather intense ($f = 0.233$) absorption for this lowest transition at 354 nm. This corresponds to the well-resolved vibronic bands at 387 and 367 nm experimentally (vibronic effects are not accounted for in the theoretical model). The next two transitions have a mixed character, with a charge transfer from the anthracene to the HBO core, and are somehow less intense (Figure S5.2). The fourth excited state is mainly located on the HBO core and is intense ($f = 0.414$). According to theory, this fourth transition has a vertical wavelength of excitation of 322 nm. The transitions to the S_2 , S_3 and S_4 states likely correspond to the broad absorption at ca. 330 nm in the experimental UV/Vis spectrum displayed in Figure 4. The relaxation of the lowest excited-state of **HBO-5-Ant** logically leads to an anthracene-based state (Figure S5.3), with a computed fluorescence wavelength of 424 nm, in good agreement with the appearance in the experimental spectrum of a vibrationally resolved emission with peaks at 407 and 425 nm (Figure 4). When starting the excited-search from a K^* structure, a second minimum can be found (see also Figure S5.3), and theory predicts an emission at 484 nm for it, again consistent with the measurements (510 nm). Though it is beyond our scope to explore the actual excited-state photodynamics of **HBO-5-Ant**, one can reasonably hypothesize the actual process.

In short, after photon absorption at 365 nm, which likely the second or third excited states, **HBO-5-Ant** has two pathways for decaying to the ground state. First, an internal conversion to the lowest excited state centered on the anthracene, which should involve a significant geometrical relaxation as the localization of the excited state changes. Second, a quick proton transfer “trapping the excited state” into a K^* state; this second path involves a more local geometrical relaxation, consistent with the difference noted between toluene and ethanol experimentally.

Conclusion

In conclusion, we have successfully optimized the Suzuki coupling conditions to introduce one or two sterically-hindered substituents on the core of ESIPT-capable HBO dyes. Depending on the nature and position of the substitution, different photophysical properties were obtained: single K^* , dual E^*/K^* or triple $E^*/D^*/K^*$ emission bands. In the solid-state, these dyes display quantum yields in the range 45–68 %, highlighting the lack of π -stacking in these compounds. Functionalization with an anthracene moiety stands out in the series, due to a strong contribution of the anthracene antenna to the overall optical properties of the dye. Future work includes coupling of these sterically-hindered groups within more complex ESIPT scaffolds.

Experimental Section

The sources of chemicals, whether any of these and/or the solvents used were purified prior to reaction, and the details (e.g., model name and number) for all instrumentation used ($^1\text{H}/^{13}\text{C}$ NMR, UV/Vis spectrophotometer, fluorimeter ...) along with full characterization of compounds are included in the Supporting Information.

5-bromo-2-(2'-Hydroxyphenyl)benzoxazole **1**,^[36] **HBO-3,5-(tBu)**₂^[37] and **HBO-3,5-(tolyl)**₂^[24] were synthesized from reported procedures.

General procedure for the synthesis of HBO-5-Mes and HBO-5-Ant: To a solution of 5-bromo HBO **1** (0.5 mmol) in DMF (20 mL) was added NaH (0.55 mmol) and Mel (0.55 mmol) and the mixture was stirred at 70 °C overnight. The reaction was then quenched with saturated NH_4Cl solution at 0 °C, taken up in CH_2Cl_2 , washed three times with saturated NH_4Cl solution, dried over MgSO_4 and concentrated *in vacuo*. The methylated HBO was then dissolved in THF (10 mL) and *t*-BuLi (1.7 M in pentane, 1 mmol) was added dropwise at –78 °C. The mixture was stirred at room temperature for 1.5 hours before the temperature was allowed to rise to 0 °C. CuI (0.55 mmol) was then added and the mixture stirred for another 30 min. Then, a solution of $\text{Pd}(\text{OAc})_2$ (0.025 mmol), tris(omethoxyphenyl)phosphine (0.075 mmol) and 2-bromomesitylene or 2-bromoanthracene (0.55 mmol) in THF (15 mL) was added *via* a cannula, keeping the temperature at 0 °C. The resulting mixture was then stirred for 4 hours at room temperature, before the solution was then taken up in CH_2Cl_2 and washed with saturated NH_4Cl solution, dried over MgSO_4 and concentrated *in vacuo*. The crude residue was purified by silica gel chromatography (petroleum ether/ CH_2Cl_2 /ethyl acetate). The purified intermediate was solubilized in CH_2Cl_2 (10 mL), before BBr_3 (1 mmol) was added to the solution at 0 °C. The resulting mixture was stirred at room temperature for 3 hours. The solution was then taken up in MeOH before it was concentrated *in vacuo*. The residue was purified by silica gel

chromatography (petroleum ether/ CH_2Cl_2) to afford HBO dyes **HBO-5-Mes** and **HBO-5-Ant** as white solids.

Suzuki-Miyaura cross-coupling reaction conditions on 3,5-dihalo-genosalicylaldehyde: In a Schlenk tube, 3,5-dihalo-genosalicylaldehyde (1 mmol.), 2,4,6-trimethylphenyl boronic acid (3 mmol.), base (3 mmol.) were dissolved in solvent (45 mL/mmol.). The resulting suspension was degassed with Argon before catalyst (5 % mol.) was added. After stirring at a given temperature, using an oil bath, crude product was analyzed by ^1H NMR and purification on silica column chromatography was performed, when the presence of salicylaldehyde **2** was detected.

Optimized synthesis of salicylaldehydes 2, 3 and 4. To a solution of 3-bromo, 5-bromo or 3,5 dibromo salicylaldehyde (1 mmol.), 2,4,6-trimethylphenyl boronic acid (1.5 for 3 and 4 or 3 mmol for 2), K_3PO_4 (3.5 mmol) in a mixture of degassed toluene/ H_2O (5 mL/1 mL) was added $\text{Pd}(\text{OAc})_2$ (0.02 mmol) and SPhos (0.04 mmol) under argon. The resulting mixture was stirred overnight at 110 °C using an oil bath. After cooling down, the solution was quenched with 2 M HCl solution, extracted with ethyl acetate, washed with brine, dried over MgSO_4 , and concentrated under vacuum. The crude residue was purified by silica gel chromatography.

General procedure for the synthesis of HBO-3,5-(Mes)₂, HBO-5-Mes and HBO-3-Mes. A mixture of salicylaldehyde **2**, **3** or **4** (0.55 mmol.) and 2-aminophenol (0.60 mmol.) were refluxed in 25 mL of ethanol for 1 hour, before the solvent was removed under vacuum to give an orange/red solid. The intermediate powder is dissolved in 100 mL of CH_2Cl_2 , and 2,6-dichloro-3,5-dicyano-1,4-benzoquinone (DDQ) (1.2 mmol), dissolved in 100 mL of CH_2Cl_2 was added dropwise. The resulting mixture was then stirred 2 hours at room temperature, before the solvents were removed under vacuum. The crude powder was purified by silica gel chromatography.

Synthesis of HBO-5-Tip. To a solution of 5-bromo HBO **1** (0.5 mmol.) in DMF (20 mL) was added NaH (0.55 mmol.) and Mel (0.55 mmol.) and the mixture was stirred at 70 °C overnight. The reaction was then quenched with saturated NH_4Cl solution at 0 °C, taken up in CH_2Cl_2 , washed three times with saturated NH_4Cl solution, dried over MgSO_4 and concentrated *in vacuo*. The crude methylated HBO (2,4,6-triisopropylphenyl)boronic acid (0.75 mmol.), K_3PO_4 (1.75 mmol.) were dissolved in a mixture of degassed Toluene/ H_2O (5 mL/1 mL), before $\text{Pd}(\text{OAc})_2$ (0.01 mmol.) and S-Bidime (0.02 mmol.) were added under argon. The resulting mixture was stirred overnight at 90 °C using an oil bath, before the solution was quenched with 2 M HCl, extracted with ethyl acetate, washed with brine, dried over MgSO_4 and concentrated under vacuum. The crude residue was first filtered on silica gel eluting with CH_2Cl_2 , before it was solubilized in 10 mL of dry CH_2Cl_2 , and a 1 M solution of BBr_3 in CH_2Cl_2 (1 mmol.) was added dropwise at 0 °C. The resulting mixture was allowed to stir at room temperature for 15 hours. The reaction was quenched with methanol over 2 hours and concentrated under vacuum. The crude residue was purified by silica gel chromatography.

Acknowledgments

The authors thank the ANR for support in the framework of the GeDeMi grant (PhD fellowship for T.P.). A.D.L. and D.J. thank the CCIPL (Centre de Calcul Intensif des Pays de la Loire) for the always generous allocation of computational time. T.S. acknowledges the ministère de l'enseignement supérieur et de la recherche for a PhD fellowship. This work of the Interdiscipli-

nary Institute HiFunMat, as part of the ITI 2021–2028 program of the University of Strasbourg, CNRS and Inserm, was supported by IdEx Unistra (ANR-10-IDEX-0002) and SFRI (STRA-T'US project, ANR-20-SFRI-0012) under the framework of the French Investments for the Future Program.

Conflict of Interest

The authors declare no conflict of interest.

Data Availability Statement

The data that support the findings of this study are available in the supplementary material of this article.

Keywords: Ab initio calculations • Fluorescence • Palladium • Catalysis • Steric hindrance

- [1] Q. J. Meisner, J. J. M. Hurley, P. Guo, A. R. Blood, R. D. Schaller, D. J. Gosztola, G. P. Wiederrecht, L. Zhu, *J. Phys. Chem. A* **2022**, 126, 1033.
- [2] J. J. M. Hurley, Q. J. Meisner, P. Guo, R. D. Schaller, D. J. Gosztola, G. P. Wiederrecht, L. Zhu, *J. Phys. Chem. A* **2022**, 126, 1062.
- [3] V. R. Mishra, C. W. Ghanavatkar, N. Sekar, *ChemistrySelect* **2020**, 5, 2103.
- [4] T. Iijima, A. Momotake, Y. Shinohara, T. Sato, Y. Nishimura, T. Arai, *J. Phys. Chem. A* **2010**, 114, 1603.
- [5] J. Zhao, S. Ji, Y. Chen, H. Guo, P. Yang, *Phys. Chem. Chem. Phys.* **2012**, 14, 25, 8803.
- [6] J. Massue, D. Jacquemin, G. Ulrich, *Chem. Lett.* **2018**, 47, 9, 1083.
- [7] V. S. Padalkar, S. Seki, *Chem. Soc. Rev.* **2016**, 45, 169.
- [8] F. G. Berbigier, L. G. T. A. Duarte, M. Fialho Zawacki, B. B. de Araújo, C. de Moura Santos, T. D. Z. Atvars, P. F. B. Gonçalves, C. L. Petzhold, F. S. Rodembusch, *ACS Appl. Polym. Mater.* **2020**, 2, 1406.
- [9] Y. Li, D. Dahal, C. S. Abeywickrama, Y. Pang, *ACS Omega* **2021**, 6, 6547.
- [10] L. G. T. A. Duarte, J. C. Germino, J. F. Berbigier, C. A. Barboza, M. M. Faleiros, D. de Alencar Simoni, M. T. Galante, M. S. de Holanda, F. S. Rodembusch, T. D. Z. Atvars, *Phys. Chem. Chem. Phys.* **2019**, 21, 1172.
- [11] J. Kumsampao, C. Chaiwai, C. Sukpattanacharoen, T. Chawanpunyawat, P. Nalaoh, P. Chasing, N. Kungwan, T. Sudyoadsuk, V. Promarak, *Mater. Chem. Front.* **2021**, 5, 16, 6212.
- [12] A. C. Sedgwick, L. Wu, H.-H. Han, S. D. Bull, X.-P. He, T. D. James, J. L. Sessler, B. Z. Tang, H. Tian, J. Yoon, *Chem. Soc. Rev.* **2018**, 47, 8842.
- [13] L. Chen, P.-Y. Fu, H.-P. Wang, M. Pan, *Adv. Opt. Mater.* **2021**, 9, 23, 2001952.
- [14] H. Sun, Y. Jiang, J. Nie, J. Wei, B. Miao, Y. Zhao, L. Zhang, Z. Ni, *Mater. Chem. Front.* **2021**, 5, 1, 347.

- [15] K. Benelhadj, W. Muzuzu, J. Massue, P. Retailleau, A. Charaf-Eddin, A. D. Laurent, D. Jacquemin, G. Ulrich, R. Ziessel, *Chem. Eur. J.* **2014**, 20, 12843.
- [16] B. Li, J. Lan, D. Wu, J. You, *Angew. Chem. Int. Ed.* **2015**, 54, 14008.
- [17] K.-C. Tang, M.-J. Chang, T.-Y. Lin, H.-A. Pan, T.-C. Fang, K.-Y. Chen, W.-Y. Hung, Y.-H. Hsu, P.-T. Chou, *J. Am. Chem. Soc.* **2011**, 133, 17738.
- [18] R. Plaza-Pedroche, M. P. Fernández-Lienres, S. B. Jiménez-Pulido, N. A. Illán-Cabeza, S. Achelle, A. Navarro, J. Rodríguez-López, *ACS Appl. Mater. Interfaces* **2022**, 14, 24964.
- [19] T. Stoerkler, T. Pariat, A. D. Laurent, D. Jacquemin, G. Ulrich, J. Massue, *Molecules* **2022**, 27, 2443.
- [20] K. Skonieczny, J. Yoo, J. M. Larsen, E. M. Espinoza, M. Barbasiewicz, V. I. Vullev, C.-H. Lee, D. T. Gryko, *Chem. Eur. J.* **2016**, 22, 7485.
- [21] J. Massue, A. Felouat, M. Curtil, P. M. Vérité, D. Jacquemin, G. Ulrich, *Dyes Pigm.* **2019**, 160, 915.
- [22] T. Pariat, M. Munch, M. Durko-Maciag, J. Mysliwiec, P. Retailleau, P. M. Vérité, D. Jacquemin, *Chem. Eur. J.* **2021**, 27, 10, 3483.
- [23] M. Munch, E. Colombain, T. Stoerkler, P. M. Vérité, D. Jacquemin, G. Ulrich, J. Massue, *J. Phys. Chem. B* **2022**, 126, 2108.
- [24] T. Pariat, T. Stoerkler, C. Diguat, A. D. Laurent, D. Jacquemin, G. Ulrich, J. Massue, *J. Org. Chem.* **2021**, 86, 17606.
- [25] E. Heyer, K. Benelhadj, S. Budzák, D. Jacquemin, J. Massue, G. Ulrich, *Chem. Eur. J.* **2017**, 23, 7324.
- [26] M. Raoui, J. Massue, C. Azarias, D. Jacquemin, G. Ulrich, *Chem. Commun.* **2016**, 52, 59, 9216.
- [27] M. Munch, M. Curtil, P. M. Vérité, D. Jacquemin, J. Massue, G. Ulrich, *Eur. J. Org. Chem.* **2019**, 1134.
- [28] M. Stolte, T. Schembri, J. Süß, D. Schmidt, A.-M. Krause, M. O. Vysotsky, F. Würthner, *Chem. Mater.* **2020**, 32, 14, 6222.
- [29] J. Gierschner, J. Shi, B. Milian-Medina, D. Roca-Sanjuan, S. Varghese, S. Park, *Adv. Opt. Mater.* **2021**, 9, 13, 2002251.
- [30] M. Oi, R. Takita, J. Kanazawa, A. Muranaka, C. Wang, M. Uchiyama, *Chem. Sci.* **2019**, 10, 6107.
- [31] A. Operamolla, O. Omar, F. Babudri, G. Farinola, F. Naso, *J. Org. Chem.* **2007**, 72, 10272.
- [32] Q. Zhao, C. Li, C. H. Senanayake, W. Tang, *Chem. Eur. J.* **2013**, 19, 2261.
- [33] M. Munch, G. Ulrich, J. Massue, *Org. Biomol. Chem.* **2022**, 20, 4640.
- [34] P. S. Nikam, B. S. Jagdale, A. B. Sawant, M. Hasan, *J. Chem. Eng. Data* **2000**, 45, 559.
- [35] Y. Inatsu, T. Arai, *Bull. Chem. Soc. Jpn.* **2014**, 87, 7, 835837.
- [36] J. Massue, T. Pariat, P. M. Vérité, D. Jacquemin, M. Durko, T. Chtouki, L. Sznitko, J. Mysliwiec, G. Ulrich, *Nanomaterials* **2019**, 9, 1093.
- [37] J. Massue, D. Frath, G. Ulrich, P. Retailleau, R. Ziessel, *Org. Lett.* **2012**, 14, 230.
- [38] C. Azarias, S. Budzak, A. D. Laurent, G. Ulrich, D. Jacquemin, *Chem. Sci.* **2016**, 7, 3763.

Manuscript received: June 3, 2022

Revised manuscript received: July 11, 2022

Accepted manuscript online: July 12, 2022